Observational constraints on the contribution of isoprene oxidation to ozone production on the western slope of the Sierra Nevada, California

Gabrielle B. Dreyfus, Gunnar W. Schade, and Allen H. Goldstein

Division of Ecosystem Sciences, Department of Environmental Science, Policy, and Management, University of California at Berkeley, Berkeley, California, USA

Received 13 November 2001; revised 5 March 2002; accepted 20 June 2002; published 1 October 2002.

[1] Observations of isoprene and its oxidation products methacrolein (MACR) and methyl vinyl ketone (MVK) are used to quantify the impact of isoprene oxidation on ozone production along the western slope of the Sierra Nevada mountains. Regular daytime up-slope wind flow patterns transport anthropogenic volatile organic compounds (VOC) and NO_x emissions from the Central Valley toward the Sierra Nevada. A north–south band of oak forests stretching along the foothills and located approximately halfway between Sacramento and our measurement site (Blodgett Forest Research Station; elevation 1315 m) injects isoprene into this mixture. Subsequently, high ozone levels are encountered in these air masses. At Blodgett, daytime mixing ratios of isoprene's oxidation products and ozone were highly correlated. The observed daytime MVK/MACR ratio was used to estimate a mean [OH] of 9 ($\pm$4) $\times$ 10^6 molec. cm^{-3} between the measurement site and the Sierra foothills. The slope of the correlation between ozone and MVK was analyzed and compared to theoretical yield ratios for the photooxidation of isoprene to estimate the fraction of total ozone production due to isoprene oxidation. On average, over 40% of the observed midday ozone formation in this region was attributable to isoprene oxidation. On ozone episode days (maximum $[O_3] > 90$ ppb), the mean isoprene contribution was over 70%. The calculated isoprene contribution to ozone production was variable from day to day but tended to increase exponentially with both isoprene input and air temperature. NO_x conditions in the up-slope air masses were very important in determining the ozone formation potential of isoprene, and the general dominance of isoprene as an ozone precursor suggests that summertime ozone abatement strategies for the region must focus on anthropogenic NO_x rather than VOC reductions. *INDEX TERMS:* 0315 Atmospheric Composition and Structure: Biosphere/atmosphere interactions; 0345 Atmospheric Composition and Structure: Pollution—urban and regional (0305); 0365 Atmospheric Composition and Structure: Troposphere—composition and chemistry

Citation: Dreyfus, G. B., G. W. Schade, and A. H. Goldstein, Observational constraints on the contribution of isoprene oxidation to ozone production on the western slope of the Sierra Nevada, California, *J. Geophys. Res.*, *107*(D19), 4365, doi:10.1029/2001JD001490, 2002.

1. Introduction

[2] Atmospheric volatile organic compounds (VOCs) play an essential role in governing the chemical processes and properties of the troposphere and the global carbon cycle [*Fehsenfeld et al.*, 1992; *Singh and Zimmerman*, 1992]. The dominant biogenically emitted VOC, isoprene (2-methyl-1,3-butadiene), reacts readily with the OH radical [*Atkinson*, 2000], and has an estimated global flux from vegetation of approximately 500 Tg C [*Guenther et al.*, 1995]. Large emission rates and high OH reactivity make isoprene particularly important in local and regional air chemistry. Ambient measurements of isoprene and its oxidation products formaldehyde (HCHO), methyl vinyl ketone (MVK), methacrolein (MACR), and 3-methyl-furan, have recently been reviewed by *Bonsang and Boissard* [1999] and *Fuentes et al.* [2000]. In general, atmospheric observations were consistent with laboratory studies of the isoprene oxidation mechanism [*Montzka et al.*, 1993, 1995; *Yokouchi*, 1994; *Biesenthal et al.*, 1997; *Starn et al.*, 1998; *Stroud et al.*, 2001]. Measurements of isoprene and its oxidation products, in particular ratios between oxidation products and their precursor isoprene, such as MVK/MACR and (MVK + MACR)/isoprene, have been used to derive information about the magnitude and location of isoprene sources on the ground [*Montzka et al.*, 1993, 1995; *Yokouchi*, 1994; *Helmig et al.*, 1998; *Stroud et al.*, 2001]. Furthermore, diurnal cycles and compound correlations at a particular site can contain information about the locally dominating oxi-

0148-0227/02/2001JD001490$09.00

dative agent, such as OH, O_3 or NO_3 [*Montzka et al.*, 1993; *Biesenthal et al.*, 1997; *Reissel and Arey*, 2001], or additional sources, such as car traffic [*Biesenthal and Shepson*, 1997].

[3] Several studies of isoprene have shown that it can contribute significantly to tropospheric ozone production in both urban and rural environments [*Trainer et al.*, 1987; *Chameides et al.*, 1988, 1992; *Biesenthal et al.*, 1997; *Starn et al.*, 1998; *Roberts et al.*, 1998; *Wiedinmyer et al.*, 2001]. Determining the contribution of biogenic VOC oxidation to ozone production in a region is key to developing an effective ozone abatement strategy because, unlike anthropogenic VOC emissions, natural emissions like isoprene are not subject to regulation [*Chameides et al.*, 1988]. From a regulatory standpoint, the importance of isoprene is compounded by the fact that the same meteorological conditions (hot and stable) that are associated with peak ozone production coincide with the conditions that produce the highest isoprene emission rates [*Goldstein et al.*, 1998]. While photochemical models have been used to investigate the effect of isoprene emissions on ozone production (reviewed by *Sillman* [1999]), few studies have determined the contribution of isoprene oxidation to ozone production based on field measurements, and most of these studies have been limited to short episodes [*Chameides et al.*, 1992; *Biesenthal et al.*, 1997; *Starn et al.*, 1998; *Roberts et al.*, 1998; *Wiedinmyer et al.*, 2001]. A commonly used method for evaluating the relative contribution of different VOCs to ozone production has been Incremental Reactivity, which is defined as the additional ozone formed given the addition of a small quantity of VOC to an existing VOC mixture in an air parcel [*Carter and Atkinson*, 1987; *Chameides et al.*, 1992; *Bowman and Seinfeld*, 1994]. Using this method and measurements of MACR to calculate reacted isoprene, *Wiedinmyer et al.* [2001] calculated ozone formation potentials from the oxidation of isoprene of up to 20 ppb under urban NO_x conditions (VOC/NO_x = 8.2) and as low as 1 ppb under rural conditions (VOC/NO_x = 20). While reactivity-weighted VOC/NO_x is useful for evaluating instantaneous ozone production, it does not provide information on integrated ozone production and transport [*Sillman*, 1999]. *Biesenthal et al.* [1997] and *Starn et al.* [1998] used concurrent measurements of ozone and isoprene's oxidation products, and theoretical ozone, MVK and MACR production yields derived from the photooxidation mechanism of isoprene to estimate the amount of ozone attributable to isoprene oxidation. This method has the benefit of directly relating observed ozone formation to inferred isoprene oxidation.

[4] While the studies listed above have shown that isoprene oxidation can be a significant source of ozone production, the factors controlling the contribution of isoprene oxidation to ozone production have not been thoroughly investigated under field conditions. In this study, we adapted the production ratio method described by *Biesenthal et al.* [1997] to estimate the contribution of isoprene photooxidation to ozone formation for individual days over two measurement seasons (~250 days with observations) at a rural site on the western slope of the Sierra Nevada Mountains, California. Regular summertime meteorological conditions allowed comparisons to be made across days and measurement seasons, providing a large data set across which to consider factors that may influence the ozone formation potential of isoprene.

2. Experiment

2.1. Site Description

[5] Blodgett Forest Research Station (38°53′42.9″N, 120°37′57.9″W, 1315 m elevation) is located on the western slope of the Sierra Nevada mountains approximately 80 km northeast of Sacramento, CA (Figure 1). A 12 m tall walk-up tower (Upright Inc.) was installed in a ponderosa pine plantation adjacent to the research station in May 1997 to investigate the biosphere–atmosphere exchange of trace gases and energy, and its effect on regional air chemistry. The land is owned and operated by Sierra Pacific Industries (SPI) and was planted with *Pinus ponderosa* L. in 1990, interspersed with a few individuals of Douglas fir, white fir, California black oak, and incense cedar. Average tree height was between 3 and 5 m in 1998 and 1999. The understory is composed primarily of manzanita (*Arctostaphylos* spp.) and whitethorn (*Ceonothus cordulatus*), however, in 1999 most of the understory was cleared during routine brush removal. Of the species observed at our site, only California black oak is a significant isoprene emitter [*Karlik and Winer*, 2001]. Details of the site and the measurement setup are described by *Goldstein et al.* [2000]. The site experiences a Mediterranean type climate, with the majority of precipitation occurring between September and May, and almost no rain in the summer. Average daily temperatures in summer 1998 ranged from 15° to 26°C, and from 11° to 22°C in 1999 (mean daily min and max). Meteorological parameters such as air temperature and humidity, wind speed and direction, and net and photosynthetically active radiation (PAR) were measured continuously and stored in 30 min averaged data sets. For a complete description of all the parameters measured, see the work of *Goldstein et al.* [2000].

[6] All instruments were housed in a temperature controlled building, and electrical power was provided by a diesel generator. The generator was located approximately 140 m northwest of the tower so as to be removed as much as possible from the main airflow paths. Contamination from generator exhaust is observed occasionally at night; however, the hydrocarbon measurements are rarely affected [*Lamanna and Goldstein*, 1999].

2.2. Measurements

[7] Continuous hydrocarbon measurements were taken at 1 hour intervals using a fully automated gas chromatograph dual flame ionization detector (GC-FID) system from July to October 1998, and from June to September 1999. In 1998, mixing ratios and vertical gradients of C_2-C_{10} VOCs were measured on two identical DB-WAX columns [*Schade et al.*, 1999]. Samples were taken simultaneously from approximately 2.5 and 4.5 m above the average tree height. The air sample preconcentration system was modified in June 1999, and two DB-624 columns were used for mixing ratio measurements until July. Then the setup was adapted for relaxed eddy accumulation (REA) measurements using a Campbell Scientific (Logan, UT) 3D sonic anemometer and data logger (CR23X) interfaced with the two-channel GC-FID equipped with two identical Rtx-WAX columns [*Schade and Goldstein*,

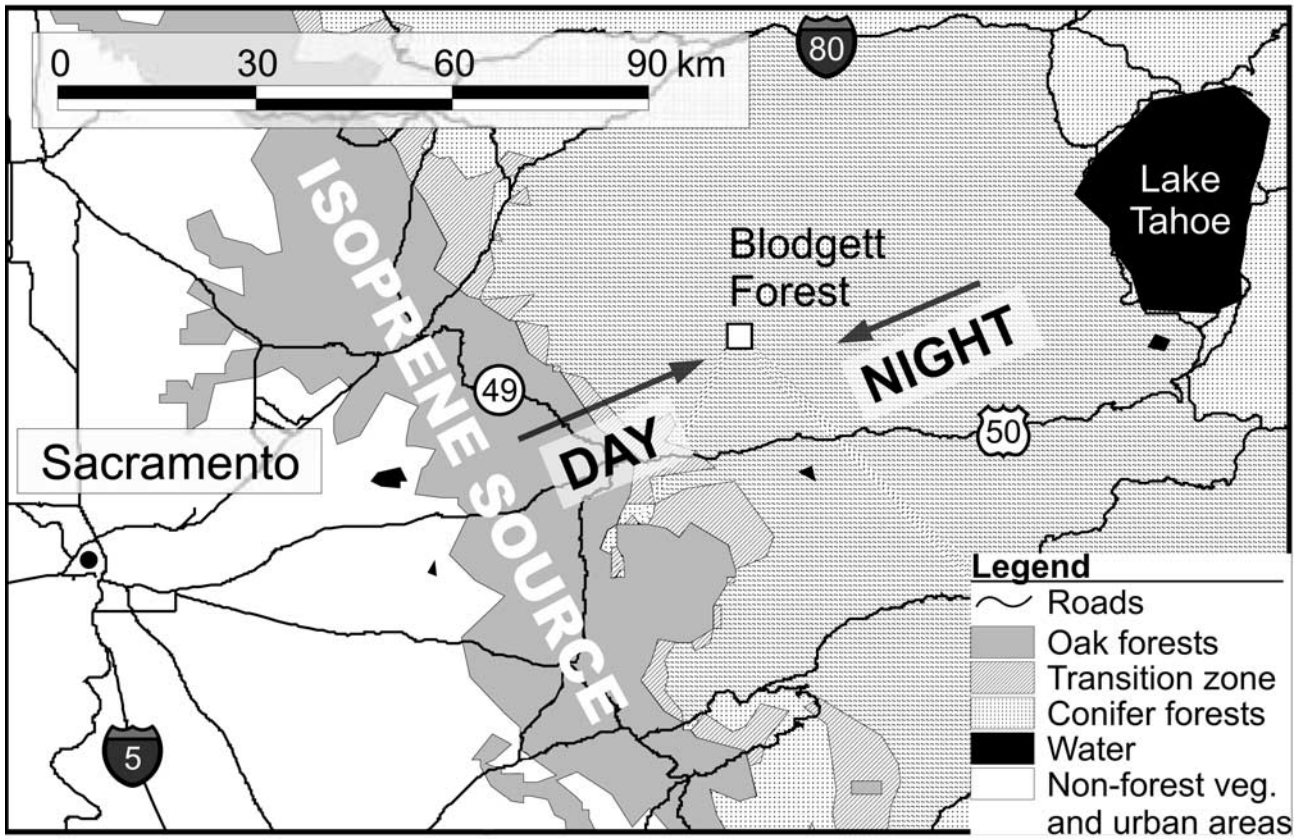

Figure 1. Map showing the regional setting and vegetation near the Blodgett Forest tower site. Arrows indicate the dominant daytime and nighttime air mass trajectories (modified from the work of *Goldstein et al.* [2000]).

2001]. Only measurements from the lower inlet (1998) and updraft samples (1999) were used for the purposes of this study. Samples in both setups were preconcentrated onto two Silcosteel© microtraps embedded in a cold-block and cooled to approximately −25°C (1998) and −10°C (1999). Sample sizes were 300 mL in 1998 (10 mL min^{-1} STP for 30 min). Sample sizes were typically <150 mL in 1999 (210 mL in June 1999 without the REA setup in place), but varied depending on the length of time the segregator valve in the REA system was "open" during the half-hour sampling period [*Schade and Goldstein*, 2001]. After collection, the samples were thermally desorbed on-column (∼250°C for 1.2 min) and detected by the two FIDs. The system was fully automated (HP Chemstation and Campbell Scientific data logger) and processed a 30 min average sample every hour. Calibration was achieved by diluting primary ppm level gas standards (Scott Marrin Inc., Riverside, CA) into the tower sampling line every 10 hours. FID response factors for compounds without standards were calculated using theoretical FID responses computed using a weighted mass percent carbon approach referenced to isoprene [*Lamanna and Goldstein*, 1999; *Schade and Goldstein*, 2001]. Isoprene and MACR were each calibrated with two different standards. MVK was not calibrated directly, but its FID response factor was assumed to equal that of MACR, since both compounds have the same carbon content and their molecular structures are similar. Detection limits for isoprene, MVK and MACR were typically 10–20 ppt. Mixing ratios above 0.2 ppb are considered accurate to ±15%. The determination limit for mixing ratio differences was estimated to be 0.2 ppb. No significant emission or deposition fluxes were detected for the compounds reported here [*Goldstein et al.*, 2001]. Calibration information data is given in Table 1 (Appendix A).

[8] Ozone mixing ratios were measured using an UV photometric analyzer (Dasibi 1008-RS), which stored averaged data every 30 min [*Bauer et al.*, 2000]. The instrument had a stated precision limit of 1 ppb, and yearly factory calibrations have shown its accuracy to be within 1%. Ambient air samples were taken at ∼5 m above average tree height at 2.5 L min^{-1} through a 2 μm filter (Zefluor, Gelman Sci.) and about 13 m of 0.635 cm Teflon tubing.

Table 1. Calibration Data for Different VOCs Measured Near Blodgett Forest Research Station

VOC	RF_{theo}[a]	RF_{meas}	DL[b] (ppb)
Isoprene	NA	0.090 ± 0.005	0.01
MACR	0.14	0.15 ± 0.01	0.015
MVK	0.14	0.15[c]	∼0.02[d]
MBO	0.11	0.11 ± 0.01	0.01
Acetone	0.21	0.20 ± 0.01	0.01

[a] RF = Response Factor (in ppb per peak area for a sample size of 150 mL). The theoretical response factor was based on a comparison to isoprene's RF.

[b] DL = Detection Limit (based on a minimum detectable peak area of 0.1, which was also approximately 3s).

[c] The MVK response factor was assumed to equal that of MACR.

[d] Chromatographic interference from benzene increased the DL for MVK.

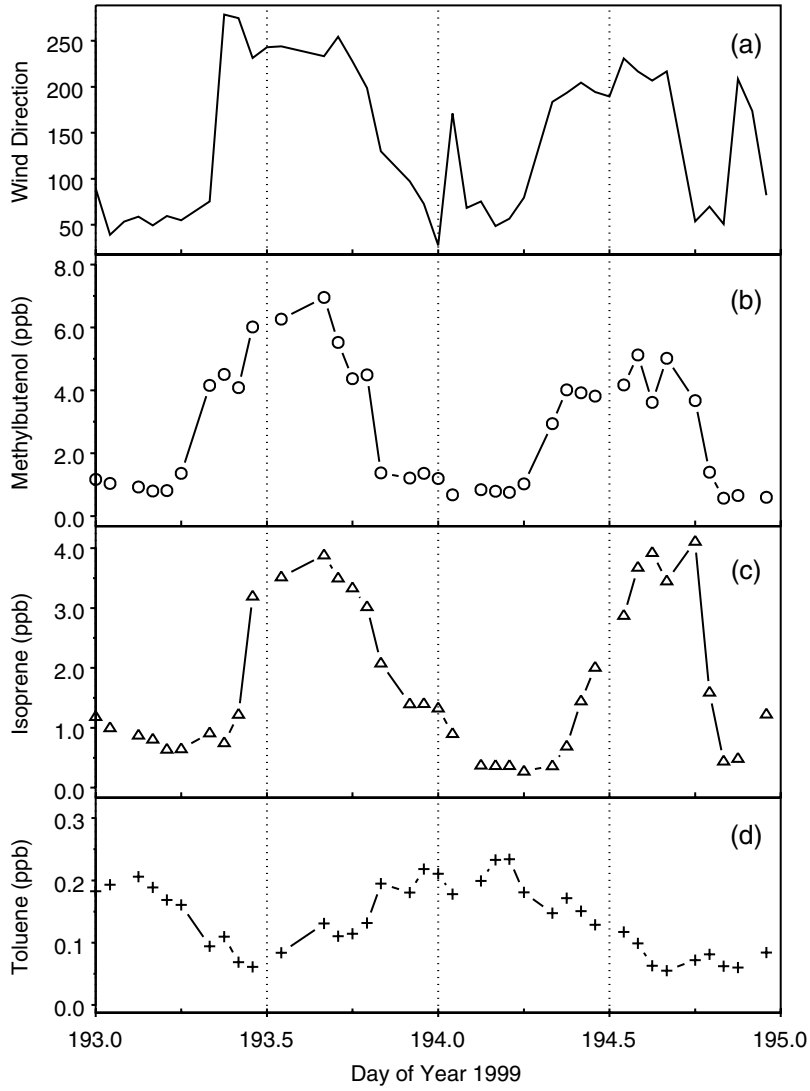

Figure 2. Two days of representative diurnal variations showing the relationship between (from top to bottom) wind direction, local biogenic (MBO), advected biogenic (isoprene), and anthropogenic (toluene) compounds.

2.3. Analytical Approach

[9] MVK and MACR are major products of the oxidation of isoprene by OH [*Tuazon and Atkinson*, 1990; *Paulson et al.*, 1992a]. In the presence of sufficient NO, ozone will also be a by-product of isoprene oxidation. If the production yields of MVK, MACR and ozone from isoprene oxidation are known, concentration–time profiles of MVK and MACR under nonsteady state conditions can be directly related to ozone production from the oxidation of isoprene [*Biesenthal et al.*, 1997; *Starn et al.*, 1998]. The fraction of total ozone production attributable to isoprene oxidation can therefore be estimated by comparing an observed increase in ozone mixing ratio (d[O_3 *total*]) to the simultaneous increases in MVK or MACR (d[MVK, MACR]):

$$\frac{\mathrm{d}[O_3\ \textit{from isop}]\Big/\mathrm{d}[\mathrm{MVK,MACR}]}{\mathrm{d}[O_3\ \textit{total}]\Big/\mathrm{d}[\mathrm{MVK,MACR}]}=\frac{\mathrm{d}[O_3\ \textit{from isop}]}{\mathrm{d}[O_3\ \textit{total}]} \quad (1)$$

where d[O_3 *from isop*] is the theoretical amount of ozone produced from the oxidation of isoprene. While the terms d[O_3 *total*] and d[MVK, MACR] are derived from measurement data, d[O_3 *from isop*] must be calculated from the ozone yield from isoprene oxidation multiplied by the total amount of isoprene oxidized. The amount of isoprene oxidized can be estimated from the measured changes in [MVK] or [MACR]. Unlike the production yields of MVK and MACR from isoprene, which have been measured under laboratory conditions, the ozone yield from isoprene oxidation is derived from the isoprene photooxidation mechanism.

3. Results and Discussion

3.1. Typical Air Mass Transport During Summer and Resulting VOC Mixing Ratio Patterns

[10] The meteorology at the Blodgett Forest tower site is characterized by a regular diurnal flow cycle driven by daytime heating and nighttime cooling in the Central

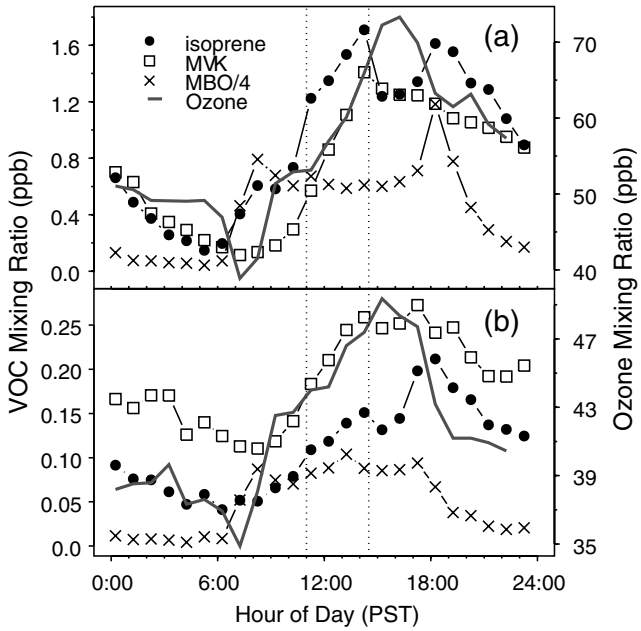

Figure 3. Mean hourly binned diurnal cycles of MBO, isoprene, its oxidation product MVK, and ozone for (a) hot (maximum temperature > 25°C) and (b) cold (maximum temperature < 20°C) days in 1998. The dotted vertical lines illustrate the period that was most commonly analyzed for the simultaneous increase in ozone and MVK.

Valley. During the day, heating in the Central Valley and along the western slope of the Sierra Nevada drives an upslope flow with winds typically blowing from the Southwest (210°–250°), which carries polluted air from the Sacramento urban area to our site [*Dillon et al.*, 2002]. At night, the wind direction reverses, ultimately bringing cleaner air down from the mountains (Figure 2a). This diurnal wind flow cycle is very consistent. It occurred on 91 out of 109 days in 1998, and on 88 out of 99 days in 1999, and is characterized by sharp wind direction shifts in the morning (typically between 0800 and 0900 Pacific Standard Time, PST) and evening (1800–1900 PST) [*Lamanna and Goldstein*, 1999]. Daytime wind speeds measured on the measurement tower ranged between 2 and 3 m s^{-1}, and were typically 0.5–1 m s^{-1} slower than speeds measured from a 45 m meteorological tower (upper wind sensor ~5 m above tree height) located on a ridgetop at Blodgett Forest Research Station (F. Schurr, personal communication, 2000), which are probably more representative of the regional flow.

[11] Anthropogenic and biogenic compounds had different diurnal mixing ratio patterns, reflecting the distance upwind of their emission sources, and the environmental parameters controlling biogenic VOC emission rates [*Lamanna and Goldstein*, 1999; *Goldstein and Schade*, 2000]. In particular, the time of mixing ratio increase after the morning wind shift was indicative of the distance from the measurement site of a compound's primary emission source. Sacramento, located in the Central Valley approximately 80 km southwest of Blodgett Forest, is the principal source of anthropogenic hydrocarbons and NO_x [*Dillon et al.*, 2002]. The land cover map in Figure 1 shows Sacramento and the regional distribution of vegetation types. Local emissions within the plantation include 2-methyl-3-buten-2-ol (MBO), several monoterpenes, and a number of oxygenated VOCs [*Schade et al.*, 1999, 2000; *Schade and Goldstein*, 2001]. As shown in Figure 2, the locally emitted MBO increases first, followed 2–3 hours later by isoprene. Anthropogenic compounds, such as toluene, increase later in the afternoon owing to the greater distance of their major sources in the Sacramento area. Some compounds, such as MVK and MACR, which are produced during transport from the isoprene source, can show a correlation with anthropogenic compounds due to coadvection [*Lamanna and Goldstein*, 1999; *Schade and Goldstein*, 2001].

[12] Oak forests and woodlands in the Sierra Nevada foothills approximately 30 km southwest of the site make up the major source of regional isoprene emissions. This is consistent with the observed 2–3 hour delay between the morning wind shift and the increases in isoprene and its oxidation products MVK and MACR (Figures 2 and 3). A comparison of the timing of the morning increases in MBO and isoprene concentration on hot (maximum temperature > 25°C) and cold (maximum temperature < 20°C) days reveals the presence of a small local isoprene source (Figure 3). The morning increase in isoprene concentration is coincident with the increase in locally emitted MBO on hot days (Figure 3a), whereas the morning increase in isoprene occurs 2–3 hours after the [MBO] increase on cold days (Figure 3b). This small local isoprene source, apparent only on hot days when isoprene emission rates are highest, can probably be attributed to a higher density of California Black Oak (*Quercus kellogii*) trees less than 0.5 km to the west and southwest of the site compared to the conifer plantations in the area. Vegetation maps also suggest populations of oaks at lower elevations between the oak forest/woodland in the foothills and Blodgett Forest that may provide an additional source of isoprene input during transport [*Goldstein et al.*, 2001]. Consequently, isoprene mixing ratios measured at Blodgett Forest are impacted by local isoprene emissions, particularly on hot days. The oxidation products we measure, however, will be more representative of the isoprene emissions from the major upwind isoprene source because

Table 2. Summary of Isoprene, MVK, and MACR Measurements for 1998 and 1999

	Isoprene (ppb)				MVK (ppb)				MACR (ppb)			
	Max	Min	Median	SD	Max	Min	Median	SD	Max	Min	Median	SD
1998 (day < 270)	3.606	<DL[a]	0.497	0.593	2.560	<DL	0.430	0.480	1.283	<DL	0.283	0.249
1998 (day > 269)	0.317	<DL	0.047	0.057	0.634	<DL	0.109	0.109	0.368	<DL	0.117	0.062
1999	4.114	<DL	0.397	0.558	4.256	<DL	0.576	0.518	2.412	<DL	0.342	0.316

[a] Detection limit (DL) is approximately 10–20 ppt.

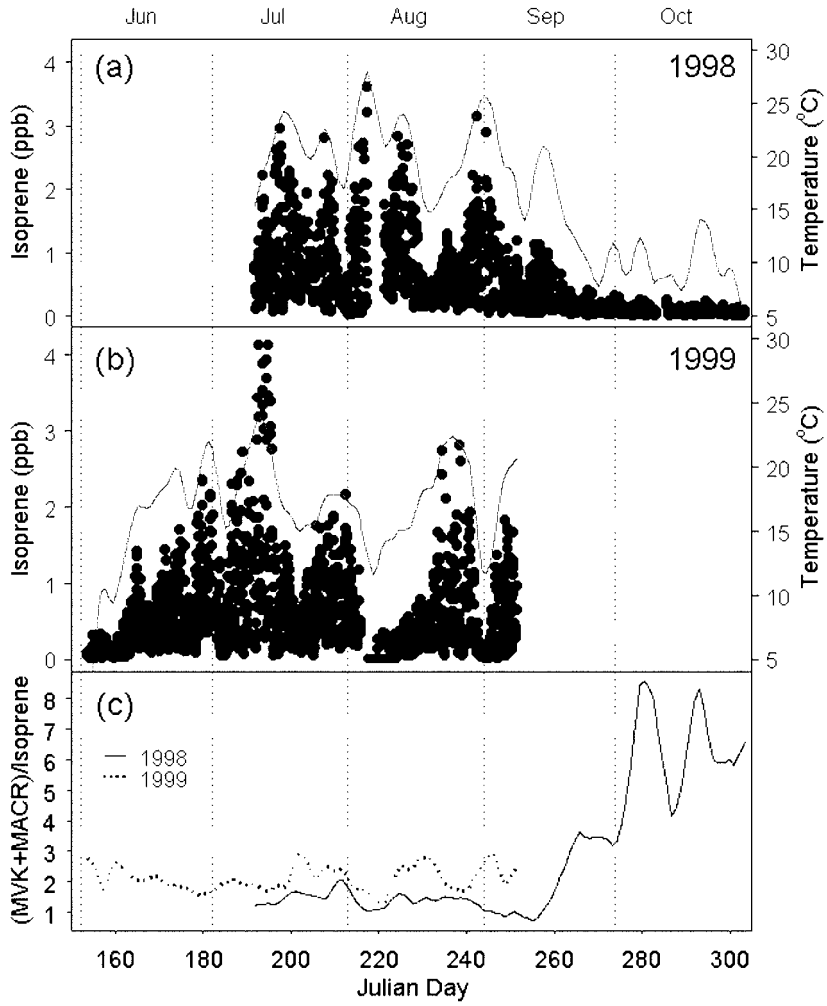

Figure 4. Measured isoprene (circles) and smoothed temperature (solid line) over the entire (a) 1998 and (b) 1999 measurement seasons. Smoothed (MVK + MACR)/isoprene for both 1998 and 1999 are shown in (c).

any local isoprene emissions will have had less time to react.

3.2. Climatology of Isoprene and its Oxidation Products

3.2.1. Abundances and Relation to Temperature

[13] Measurements of isoprene and its oxidation products MVK and MACR were taken from 12 July to 31 October 1998 and 2 June to 8 September 1999, and are summarized in Table 2. Measurements of isoprene and air temperature over the entire 1998 and 1999 measurement seasons are shown in Figure 4. As isoprene emissions increase with PAR and temperature [*Guenther et al.*, 1993; *Goldstein et al.*, 1998; *Fuentes et al.*, 2000], an exponential relationship between ambient isoprene near the ground and air temperature is often found [e.g., *Guenther et al.*, 1993; *Goldan et al.*, 1995]. This exponential relationship between daytime isoprene mixing ratios and temperature was evident during the summer months of both the 1998 and 1999 measurement periods (Figure 5). A log linear fit of isoprene against temperature (°C) for both 1998 and 1999 gave a relationship of exp(0.189 × T) with a coefficient of determination, r^2, of 0.74. This is similar to the exponential dependence of exp(0.174 × T) found by *Goldan et al.* [1995] at both the Scotia, Pennsylvania, site in 1988, and the Kinterbish Wildlife Management Area, Alabama, in 1990. Besides temperature, tree phenology on a seasonal timescale is also an important factor determining isoprene emissions [*Goldstein et al.*, 1998]. As shown in Figure 4, isoprene concentrations in 1998 decreased sharply around day 260 with the beginning of leaf senescence in fall.

[14] The correlation between isoprene's oxidation products and temperature for the full measurement period (r^2 = 0.42 for 1998 and 1999) was not as strong as for isoprene itself. This feature was noted before by *Montzka et al.* [1995], pointing out that as both MVK and MACR are produced in the boundary layer, their mixing ratios are more subject to dynamic influences such as boundary layer height.

[15] Throughout both measurement seasons, MVK and MACR were very highly correlated with one another, and well correlated with isoprene, especially during times of SW-wind direction (Figure 6). The correlation with isoprene

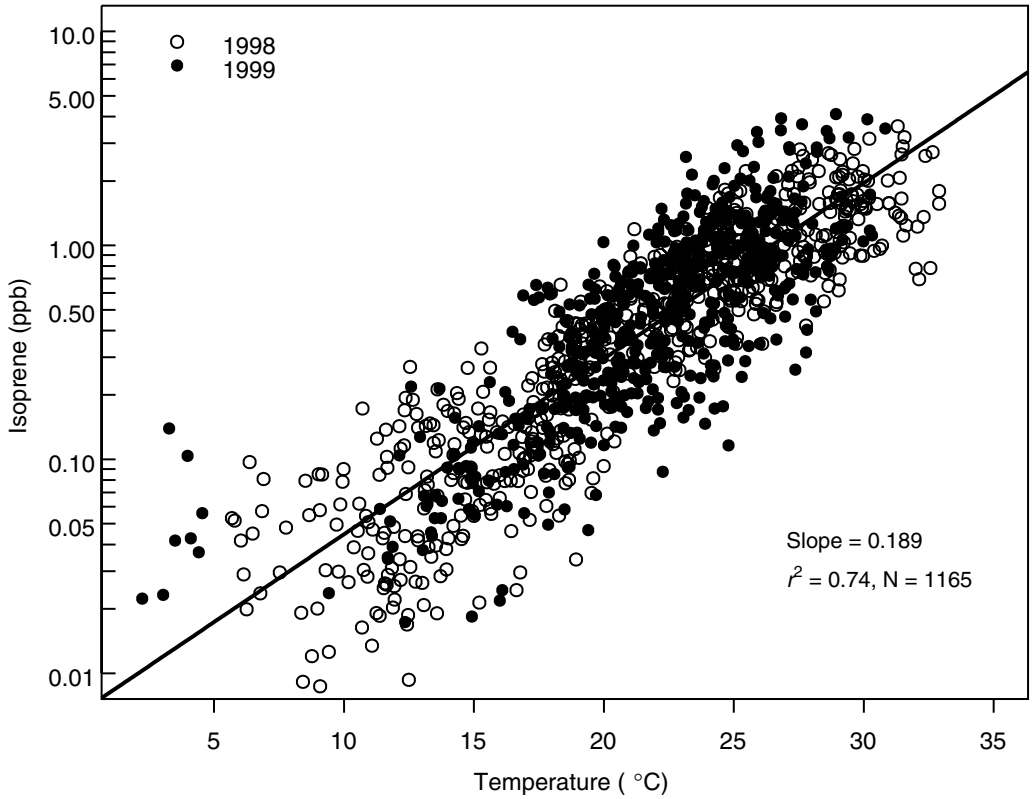

Figure 5. Relationship between daytime isoprene and air temperature (0900–1700 PST and 200°–300° wind direction sector).

was often broken early in the morning due to local isoprene emissions. Comparison of the diurnal patterns of hourly binned isoprene, MVK, MBO and ozone on hot days (Figure 3a) and cold days (Figure 3b) shows that local isoprene emissions are most apparent on hot days, but are too small to be detected on cold days. Notice also the difference in magnitude between the hydrocarbon and ozone mixing ratios on hot and cold days. As illustrated by Figure 7a, isoprene and its oxidation products exhibited similar diurnal mixing ratio patterns with minima around 0700 PST, strong increases starting at 1000 PST (2–3 hours after the morning wind direction shift), and peak concentrations occurring approximately 4 hours later. MVK and MACR concentrations stayed level or declined slowly throughout the afternoon and into the evening, while isoprene levels had a second smaller evening peak around 1900 PST. These diurnal trends were similar to those recorded over a rural forested site with significant local isoprene emissions in western Alabama (ROSE) [*Montzka et al.*, 1993, 1995; *Goldan et al.*, 1995], with several important differences. MVK and isoprene mixing ratios measured at our site were of comparable magnitude throughout the day, while the isoprene concentrations measured at the ROSE site were 5 times greater than MVK [*Montzka et al.*, 1993]. The morning increases in MVK and isoprene concentrations started at 6 AM local time (CST) for *Montzka et al.* [1993], approximately 4 hours before the increase recorded at our site. Isoprene mixing ratios continued to increase throughout the day at the ROSE site, with maximum concentrations occurring in the early evening around sunset. These are differences that would be expected given the presence of significant local isoprene sources at the ROSE site, while our site is approximately 30 km downwind from the region's major isoprene source.

3.2.2. MVK/MACR Ratio

[16] The MVK/MACR ratio measured at our site showed a diurnal pattern very similar to that found by *Montzka et al.* [1993] and *Stroud et al.* [2001], with values around 2 during the day, and decreasing down to 1 during the night and into the early morning (Figure 7b). As shown in Tables 3 and 4, MVK and MACR have distinct production ratios depending on the isoprene oxidant, and in addition, have different reaction rates with OH and ozone. In light of these properties, the MVK/MACR ratio can be used to determine the dominant oxidant in an air mass. Oxidation of isoprene by OH in the presence of NO produces MVK and MACR in a ratio of approximately 3:2, whereas oxidation of isoprene by ozone yields the reverse production ratio of 2:3. During the day, when OH is the dominant oxidant, we expect to see an MVK/MACR ratio of at least ~1.4 (Table 3). This is the initial MVK/MACR yield ratio from the oxidation of isoprene by OH in the presence of NO, and we expect the ratio to increase with additional oxidation because MVK has a longer lifetime than MACR with respect to reaction with OH. The observed diurnal pattern with a daytime ratio around 2 and nighttime ratio around 1, therefore, indicates that OH chemistry dominates during the day, and ozone chemistry and dilution are driving the observed nighttime ratio.

[17] Two recent laboratory studies (Table 3), and a modeling study [*Jenkin et al.*, 1998], have pointed out that

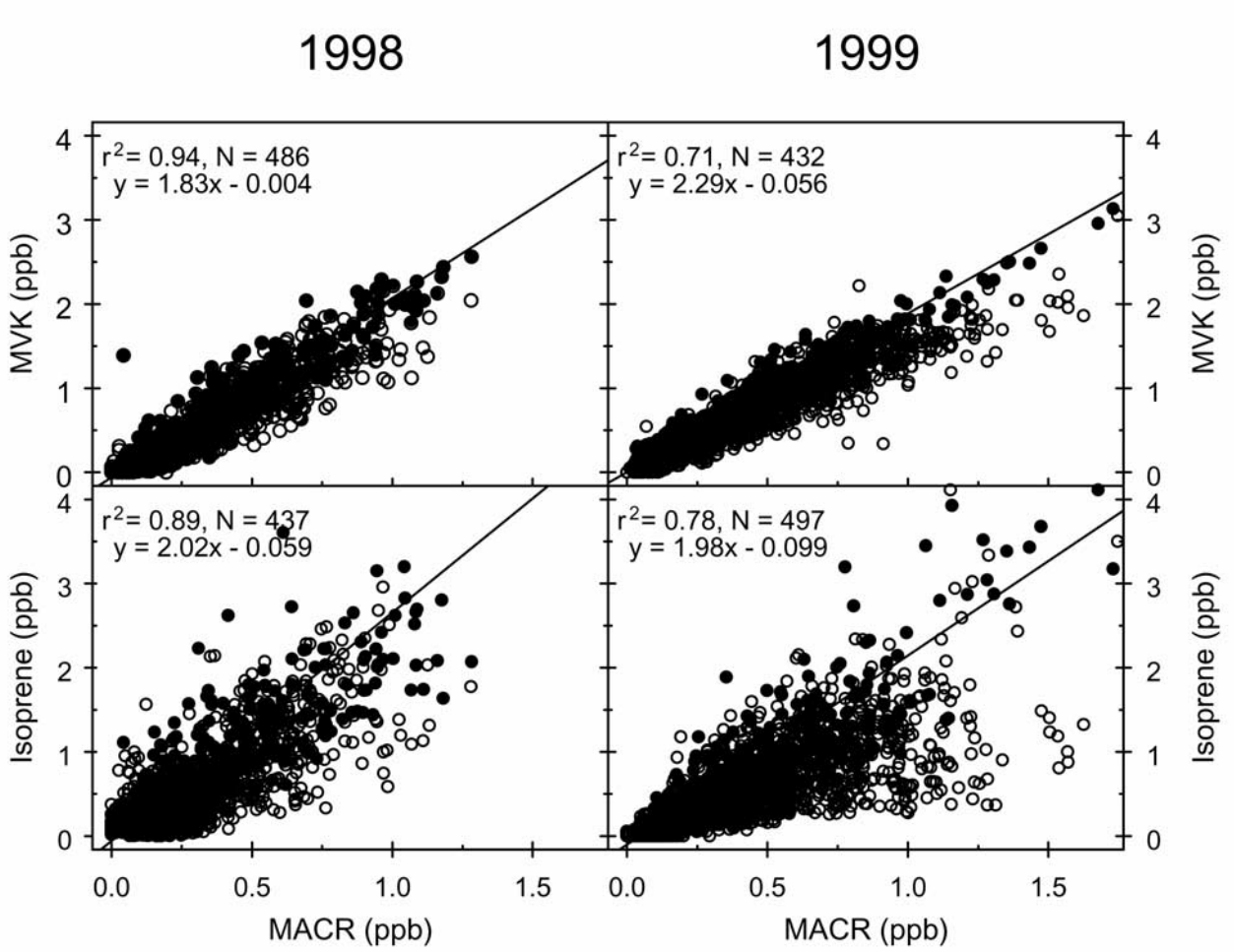

Figure 6. Correlations between oxidation products and isoprene for 1998 and 1999. Open circles are all points. Filled circles are for daytime data only (0900–1700 PST and 200°–300° wind direction sector), and the lines are mutual least squares fits of those.

MVK and MACR yields from the oxidation of isoprene by OH depend on NO availability. Consequently, these changes may have to be taken into account when interpreting the MVK/MACR ratio measured in regions with low NO_x mixing ratios. As will be discussed below, the peroxy radicals produced from the oxidation of isoprene and other VOCs can react with one another rather than with NO, creating new pathways that compete with the MVK and MACR forming pathways, thereby resulting in reduced MVK and MACR yields. For the case shown in Figure 7a, decreased isoprene emission, high upwind (midday) OH and/or high peroxy-radical levels are possible reasons for the decline of MVK and MACR mixing ratios after 1400 PST. Increasing [OH] is probably not the reason for the decrease in MVK and MACR mixing ratios during this time of day because [OH] should decrease in the afternoon as radiation inputs decrease. A comparable afternoon decrease, though less pronounced, was observed over the ROSE site, another rural forested site [*Montzka et al.*, 1993, 1995], but not by *Stroud et al.* [2001] in an urban region. Despite these differences, all three sites showed very similar trends in diurnal mean MVK/MACR, again underlining that the diurnal MVK to MACR ratio is governed by OH chemistry.

[18] Both at our and at the ROSE site, a leveling or even a drop in the MVK to MACR ratio was observed several hours before sunset (Figure 7b). There are two possible reasons for this decrease: decreasing [OH] or a significant change in the MVK to MACR production yield ratio. If [OH] levels were decreasing alone, without an accompanying decrease in isoprene emissions, we would expect to see an increase in [MVK] and [MACR] during this time. As this is not the case (Figure 7a), either isoprene emissions must also be decreasing, or competition due to high peroxy-radical mixing ratios must be present. As the former would input less MVK and MACR at a production ratio of $\leq$1.4, which would lead to an increase in the resulting MVK to MACR ratio, high peroxy-radical mixing ratios remain as the likely reason for the afternoon MVK to MACR ratio decrease. At the ROSE site, this is consistent with low NO_x, high measured RO_x and isoprene mixing ratios, but moderate ozone mixing ratios that do not continue to increase in the afternoon [*Frost et al.*, 1998], wherefore [OH] is expected to drop. Hence, both high RO_x and decreasing [OH] could be driving the afternoon MVK to MACR decrease at the ROSE site. At our site, high OH radical levels have been estimated upwind [*Dillon et al.*, 2002], and ozone values keep increasing into the late afternoon (Figure 3) [*Bauer et al.*, 2000], wherefore [OH] levels

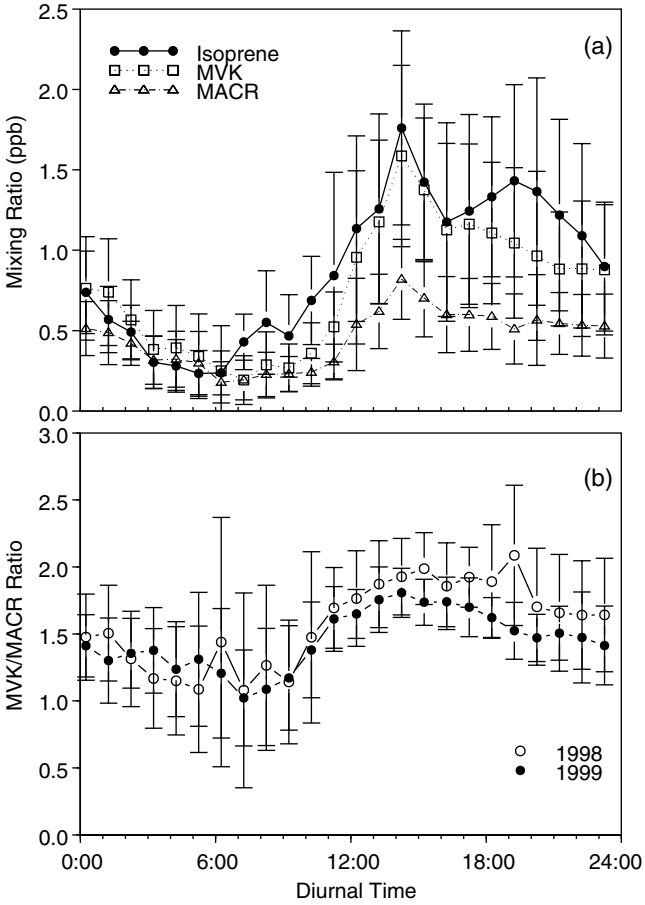

Figure 7. Mean hourly binned diurnal (a) isoprene, MVK, and MACR mixing ratios for July 1998 and (b) MVK/MACR ratio for July 1998 and 1999. Vertical bars represent one standard deviation.

are not expected to drop very significantly. Thus, we conclude that a likely reason for the afternoon MVK to MACR ratio decrease at our site is indeed an increase in peroxy-radical competition, reducing the MVK to MACR production ratio.

[19] In contrast to the above sites, high NO_x, ozone and OH radical values prevailed at the Cornelia Fort Airport site [*Stroud et al.*, 2001], and, together with an average transport time of 1.6 hours, high-NO_x and high [OH] chemistry is able to explain both the daytime decrease of MVK and

Table 3. Reported Yields of MVK and MACR From the OH-Initiated and O_3-Initiated Oxidation of Isoprene

	OH-initiated oxidation pathway			
	HCHO (% yield)	MVK (% yield)	MACR (% yield)	NO_x condition
Tuazon and Atkinson [1990]	50 ± 10	29 ± 7	21 ± 5	high
Paulson et al. [1992a]	67 ± 7	35.5 ± 4	25 ± 3	high
Miyoshi et al. [1994]	57 ± 6	32 ± 5	22 ± 2	high
Ruppert and Becker [2000]	57 ± 6	31 ± 3	20 ± 2	high
Miyoshi et al. [1994]	34	17	22	free
Ruppert and Becker [2000]	33 ± 3	15.3 ± 1.2	17.8 ± 1.4	free
	O_3-initiated oxidation pathway			
Paulson et al. [1992b]		26 ± 6	67 ± 9	NO_x free
Grosjean et al. [1993]	90	17	44	NO_x free

Table 4. Reaction Rate Constants and Lifetimes of Isoprene, MVK, and MACR

Compound	k_{OH}	τ^a, hours	k_{O3}	τ^a, hours
Isoprene	1.01×10^{-10}	0.21–0.55	1.28×10^{-17}	17
MVK	1.88×10^{-11}	1.1–3.0	4.56×10^{-18}	48
MACR	3.35×10^{-11}	0.6–1.7	1.14×10^{-18}	193

[a] Lifetimes assuming [OH] = $9 \pm 4 \times 10^6$ molec. cm^{-3}; [O_3] = 60 ppb. Reaction rates from the work of *Atkinson et al.* [2000].

MACR mixing ratios and the observed MVK to MACR ratio (~1.9) in the afternoon, including its decrease with [OH] after sunset.

3.3. Ozone

[20] Mean daytime ozone mixing ratios in the summer typically ranged from 40 to 90 ppb in 1998 and 1999. In 1998, daytime mean ozone concentrations after day 260 (18 September 1998) were generally lower, ranging from 28 to 66 ppb. According to our measurements, daytime ozone concentrations exceeded the California Ambient Air Quality Standard of over 90 ppb for 1 hour on 5 days during our measurement period in 1998 (days 198, 200, 223, 224, and 246), and on 21 measured days in 1999 (days 157, 168, 187, 191–195, 203, 204, 207–209, 211, 228, 229, 236, 237, 240, 241, and 250). Ozone mixing ratios generally showed a diurnal pattern with a morning minimum around the time of the morning wind shift, and a maximum in the late afternoon (Figure 3). The morning dip in ozone is caused by increased deposition to the canopy as the trees become active at sunrise while the nocturnal inversion layer is still present [*Bauer et al.*, 2000].

3.4 Relating Ozone and Isoprene Oxidation Product Measurements

[21] Most days under normal wind conditions showed a period of simultaneous increase in MVK, MACR, and ozone for 3–5 hours in the middle of the day (Figure 3). By comparing the slope of the changes in the observed [O_3] to the changes in the observed [MVK] or [MACR] (d[O_3 *total*]/d[MVK, MACR]) to the production ratio calculated from the oxidation mechanism of isoprene, we can estimate the fraction of total ozone production attributable to isoprene (equation (1)).

[22] Individual days and time windows for analysis were selected to capture this period of concurrent increase, according to the following five criteria: (1) only days that demonstrated a clear morning wind direction shift and daytime wind direction between 190° and 300° were considered. This wind direction sector was defined to select for air masses with similar trajectories from the Sacramento valley to the measurement site via the Sierra foothills. Air masses arriving from this sector should have experienced similar NO_x and isoprene inputs. (2) Only clear-sky or partially cloudy days were evaluated. Days with mean midday PAR less than 50% of potential PAR were excluded because cloudy conditions affect the rates of NO_2 photolysis, OH production, and isoprene emission. (3) A time window for analysis was selected for each day such that the window began at least 2 hours after the morning wind direction shift, and ended when MVK and MACR mixing ratios leveled off, but never more than 5 hours after the start of the time window. The morning limits on the time windows were

Table 5. Number of Days in 1998 and 1999 That Met the Selection Criteria for Analysis of the Contribution of Isoprene Oxidation to Ozone Formation

	Measurement days	Norm WD[a]	Sunny	$N > 2$	$r^2 > 0.64$	Flagged days[b]
1998						
July	22	21	21	17	9	0
August	28	27	27	23	14	1
September	30	25	25	24	14	1
October	29	19	18	12	7	5
Total	109	92	91	76	44	7
1999						
June	29	27	25	17	11	1
July	31	27	27	24	16	0
August	31	27	27	19	15	2
September	8	7	7	6	4	0
Total	99	88	86	66	46	3

[a] Normal wind direction pattern (see text).
[b] Days with changes in [MVK] < 0.2 ppb or [O_3] < 2 ppb over the analyzed time period were flagged and dealt with separately.

selected to ensure that all observed air masses had sufficient time to get from the isoprene source to the measurement site. After 5 hours, the correlation between ozone and isoprene's oxidation products was lost on most days (Figure 3), possibly due to the build up of peroxy radicals in the afternoon. This effect is considered in the following section. (4) Three simultaneous observations of MVK and ozone were required for each chosen time window. While ozone to MACR slopes were calculated for days with sufficient MACR, the relationship between MVK and ozone was the primary focus of this analysis. (5) Days exhibiting increases in MVK or ozone below the instrument determination limits of 0.2 and 2 ppb, respectively, were flagged and treated separately, as described below. Excluding these discriminates against days with low isoprene input, and hence, low isoprene contribution. Consequently, days with greater isoprene contribution would be preferentially selected. A summary of the data selection is given in Table 5.

[23] The slope of the ozone increase over the concurrent MVK or MACR increase was calculated using mutual least squares regression for each day that met the above selection criteria. This analytical approach assumes simultaneous formation of ozone and isoprene oxidation products from the oxidation of isoprene in a given air mass, and can only be used in situations where ozone, MVK, and MACR are well correlated. Processes such as mixing and dilution can alter the ozone to MVK correlation, and the effect of such processes on this analysis will be considered below. A minimum correlation coefficient of 0.8 ($r^2 > 0.64$) was adopted to exclude such days. Given this r^2 limit, the calculated ozone to MVK slopes (excluding flagged days in parentheses) were still found to be highly variable, ranging from 5 ± 1 to 302 ± 31 (70 ± 10) with a median of 27 (18) in 1998, and 4.0 ± 0.1 to 119 ± 15 (78 ± 38) with a median of 17 (17) in 1999, where the reported uncertainties are the standard error of each regression. The ozone to MACR slopes ranged from −290 to 999 in 1998; however, this range reduced to 4 ± 6 to 415 ± 200 (197 ± 135) with a median of 63 (56) when 8 days with only 2 MACR measurements were excluded. In 1999 ozone to MACR slopes ranged from 9 ± 7 to 488 ± 648 (215 ± 147) with a median of 45 (40). The slopes of d[O_3 *total*]/d[MVK] and d[O_3 *total*]/d[MACR] were well correlated ($r^2 = 0.60$, N = 81 for combined 1998 and 1999, including flagged days, but excluding 9 days with only 2 MACR measurements), and had the relationship predicted by the mechanism of isoprene, MVK and MACR oxidation (d[MVK]/d[MACR] = 2.1 ± 0.2). The calculated d[O_3 *total*]/d[MVK] slopes are shown in Figure 8 plotted against the total change in [MVK] over the period of concurrent [MVK] and [O_3] increases for each day. The amount of isoprene oxidized over this period should be proportional to the total change in MVK over this period under nonsteady state conditions. The contribution of isoprene oxidation to ozone production is expected to increase as more isoprene is oxidized. The calculated d[O_3 *total*]/d[MVK] was found to decrease with increasing isoprene oxidized, but did not drop below a lower limit of approximately 5 (Figure 8). As will be discussed below, this behavior is consistent with isoprene becoming the dominant ozone precursor. The observed ratio of total ozone production per isoprene oxidized should approach the ozone yield from isoprene as isoprene oxidation becomes the dominant source of ozone production (equation (1)).

3.5. NO_x Dependence of Isoprene Chemistry

[24] The contribution of isoprene oxidation to ozone production can only be calculated if the production yields of MVK, MACR and ozone from the oxidation of isoprene are known. As summarized in Table 3, laboratory studies have found that MVK and MACR yields were different under high-NO_x and NO_x-free experimental conditions. In addition, the production yield of ozone from isoprene oxidation is also highly dependent on NO_x availability [*Trainer et al.*, 1987; *Sillman et al.*, 1990; *Starn et al.*, 1998; *Sillman*, 1999; *Wiedinmyer et al.*, 2001]. In the following discussion we use the isoprene photooxidation mechanism to explore the NO_x dependence of the MVK, MACR and ozone production yields, and estimate appropriate yields under our field conditions.

[25] The production of MVK, MACR and ozone from the OH-initiated oxidation of isoprene can be summarized by the following reaction pathway:

$$\mathrm{ISOP + OH + O_2 \rightarrow ISOP - OO + H_2O} \quad (2)$$

$$\mathrm{ISOP - OO + NO \rightarrow ISOP - O + NO_2} \quad (3a)$$

$$\rightarrow \mathrm{ISOPONO_2} \quad (3b)$$

$$\mathrm{ISOP - O + O_2 \rightarrow MVK + HCHO + HO_2} \quad (4a)$$

$$\rightarrow \mathrm{MACR + HCHO + HO_2} \quad (4b)$$

$$\rightarrow \mathrm{products + HO_2} \quad (4c)$$

$$\mathrm{HO_2 + NO \rightarrow OH + NO_2} \quad (5)$$

$$\mathrm{NO_2 + h\upsilon + O_2 \rightarrow O_3 + NO} \quad (6)$$

[26] The ozone yield is equivalent to the number of NO_2 produced per isoprene oxidized, since NO_2 photolyzes rapidly to produce ozone during the day. NO_2 is produced directly in reaction (3a), and in reaction (5) for each

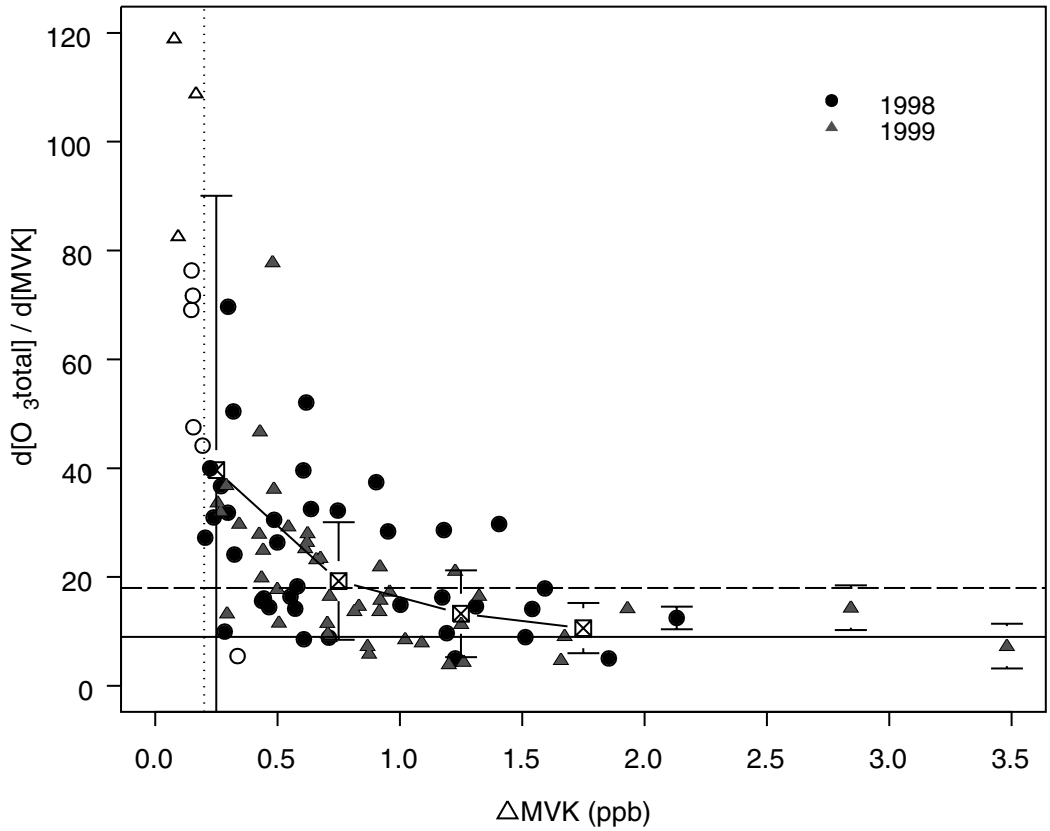

Figure 8. The slope of the change in ozone over the change in MVK (d[O_3 *total*]/d[MVK]) is calculated for individual days during periods of concurrent increases in [O_3] and [MVK] (see Figure 3). These slopes are plotted against the total change in [MVK] for the period of concurrent increase, where the total change in [MVK] serves as a proxy for the amount of isoprene oxidized. The crossed boxes represent binned average slopes with standard errors. Error bars on single points represent the uncertainty of the calculated slope for that day. Open symbols are ''flagged days'' (see text).

isoprene-derived HO_2 from reactions (4a), (4b), and (4c) that reacts with NO. The ozone production yield can therefore be expressed as:

$$\frac{\mathrm{d}[O_3\ \textit{from isop}]}{\mathrm{dt}} = \left(\frac{k_{3a}}{k_{3a}+k_{3b}}\right) R3 + R5 \qquad (7)$$

where we assume a branching ratio for reactions (3a) and (3b) of $k_{3a}/(k_{3a} + k_{3b}) = 0.95$, which may be an underestimation. Published estimates for the formation of isoprene-nitrates range from 4.4% [*Chen et al.*, 1998] to 8–13% [*Tuazon and Atkinson*, 1990]. However, using measurements of isoprene nitrates, *Grossenbacher et al.* [2000] found that isoprene nitrate formation is NO_x dependent, and may be even smaller than published estimates under low-NO_x conditions.

[27] Under low-NO_x conditions, peroxy-radical reaction with HO_2 and RO_2 cross-reactions can compete with reactions (3a) and (3b):

$$\mathrm{ISOP-OO} + \mathrm{HO_2} \rightarrow \mathrm{ISOP-OOH} + \mathrm{O_2} \qquad (8)$$

$$\mathrm{ISOP-OO} + \mathrm{RO_2} \rightarrow \mathrm{ISOP-O} + \mathrm{RO} + \mathrm{O_2} \qquad (9a)$$

$$\rightarrow \mathrm{ISOP-OH} + \mathrm{carbonyl} + \mathrm{O_2} \qquad (9b)$$

where $k_3 \approx 9 \times 10^{-12}$ cm^3 molec.$^{-1}$ s^{-1} (at 295 K) (uncertainty factor of 2) [*Stevens et al.*, 1999; *Atkinson*, 2000], $k_8 \approx 1.6 \times 10^{-11}$ cm^3 molec.$^{-1}$ s^{-1} (at 295 K) (uncertainty factor of 2) [*Jenkin et al.*, 1998; *Atkinson*, 2000], $k_9 \approx 4 \times 10^{-12}$ cm^3 molec.$^{-1}$ s^{-1} [*Ruppert and Becker*, 2000 (adapted from *Jenkin et al.* [1998])], and $k_{9a}/k_9 = 75 \pm 7\%$ [*Ruppert and Becker*, 2000]. A modeling study has shown that reactions (3a) and (3b) will dominate for [NO] > 30 ppt, and that reaction with HO_2 will dominate at lower NO concentrations [*Logan*, 1985]. More recently, organic peroxy-radical self- and cross-reactions (reactions (8) and (9a) and (9b) for isoprene) have been estimated as a significant reaction pathway under low NO_x conditions. *Ruppert and Becker* [2000] estimated that up to 20% of peroxy radicals undergo cross-reactions at NO levels of 60–250 ppt and peroxy-radical mixing ratios of 25–50 ppt, based on rate constant estimates by *Jenkin et al.* [1998].

[28] Measured daytime NO mixing ratios at our site were generally above 50 ppt, and are expected to be higher than 100 ppt 30 km upwind, closer to the major NO_x sources in the Central Valley [*Dillon et al.*, 2002]. While total peroxy-radical concentrations were not measured, midday total [RO_2] + [HO_2] mixing ratios are expected to range between 50 and 100 ppt, with an estimated RO_2/HO_2 ratio of at least 3 [*Stevens et al.*, 1997]. The range is similar to that measured in the ROSE oxidant study [*Cantrell et al.*, 1993], which was characterized by biogenic hydrocarbon emissions similar in composition and magnitude to those at our site [*Goldan et al.*,

1995]. Given this expected range in NO (100–250 ppt) and peroxy radicals ($[RO_2] + [HO_2] = 50–100$ ppt) upwind of our site, competing peroxy-radical reactions will be significant; however, the exact portion of isoprene peroxy-radicals reacting with NO as opposed to RO_2 or HO_2 is uncertain and probably highly variable from one day to the next.

[29] For the purposes of this analysis, we selected two representative NO_x scenarios, defined in terms of γ, the fraction of isoprene-derived peroxy radicals (ISOP-O_2) that reacts with NO [*Barket et al.*, 2000]:

$$\gamma = \frac{k_3[\mathrm{NO}]}{k_3[\mathrm{NO}] + k_9[\mathrm{RO_2}] + k_8[\mathrm{HO_2}]} \quad (10)$$

A similar term can be defined for the fraction of HO_2 that reacts with NO. Under our experimental conditions, we find that this term is approximately equivalent to γ. Hence, for the purposes of this analysis, we will use a single value of γ to represent the fraction of both ISOP-O_2 and HO_2 reacting with NO.

[30] The first scenario we consider is a "high-NO_x" condition, defined as $\gamma = 1$, where all peroxy radicals react with NO. Second, we define a "low-NO_x" scenario as $\gamma = 0.5$, and we assume that approximately 30% of all isoprene peroxy-radicals that do not react with NO will undergo cross-reactions to produce alkoxy radicals (ISOP-O), which can react with O_2 to produce HO_2 (4), MVK and MACR. This characterization for a low-NO_x condition is similar to calculations by *Grossenbacher et al.* [2000] of a γ between 0.4 and 0.9 for a NO_x level of around 1 ppb, and estimates by *Biesenthal et al.* [1998] that approximately half of the isoprene peroxy-radicals would react with NO at NO levels of 50 ppt and peroxy-radical mixing ratios of 20–40 ppt.

[31] As stated in equation (7), ozone production depends on the rates of reactions (3a) and (5), and can be expressed in terms of γ as follows:

$$\frac{\mathrm{d}[\mathrm{O_3}\ \textit{from isop}]}{\mathrm{dt}} = \gamma \times \mathrm{R2} \times \left(\frac{k_{3a}}{k_{3a} + k_{3b}}\right) + \gamma \times \mathrm{R5} \quad (11)$$

Where we have assumed that ISOP-O_2 and HO_2 are in steady state. The rate of reaction (5) is equal to the rate of formation of the isoprene alkoxy radical from reactions (3a) and (9a):

$$\mathrm{R5} = \left(\frac{k_{3a}}{k_{3a} + k_{3b}}\right)\mathrm{R3} + \left(\frac{k_{9a}}{k_{9a} + k_{9b} + k_{9c}}\right)\mathrm{R9} \quad (12)$$

and

$$\left(\frac{k_{9a}}{k_{9a} + k_{9b} + k_{9c}}\right)\mathrm{R9} = \mathrm{R2} \times (1 - \gamma) \times \frac{k_{9a}[\mathrm{RO_2}]}{k_8[\mathrm{HO_2}] + k_9[\mathrm{RO_2}]} \quad (13)$$

[32] Substituting back into equation (11) and using the values $k_{3a}/(k_{3a} + k_{3b}) = 0.95$ and $k_{9a}[RO_2]/(k_9[RO_2] + k_8[HO_2]) = 0.3$ gives:

$$\frac{\mathrm{d}[\mathrm{O_3}\ \textit{from isop}]}{\mathrm{dt}} = \mathrm{R2} \times [0.95 \times \gamma + \gamma \times (0.95 \times \gamma + (1 - \gamma) \times 0.3)] \quad (14)$$

Using equation (14), we calculate an ozone yield per isoprene oxidized under "high-NO_x" conditions ($\gamma = 1$) of 1.9, analogous to the yield of 1.76 calculated by *Biesenthal et al.* [1997], who assumed an alkyl-nitrate formation rate of 12%. The ozone yield under "low-NO_x" conditions (here defined as $\gamma = 0.5$) is only 0.79.

[33] While laboratory measurements of the MVK and MACR yields from the OH-initiated oxidation of isoprene have been made under high- and NO_x-free conditions (Table 3), such measurements have not been made under the NO_x conditions expected at this site. The lower yields under NO_x-free conditions have been attributed to the slow cross-reactions of secondary and tertiary peroxy-radical intermediates that form the alkoxy radical precursors to MVK and MACR [*Paulson et al.*, 1992b; *Miyoshi et al.*, 1994]. The MVK and MACR yields under low-NO_x conditions should therefore depend on the fraction of peroxy-radical intermediates that react with NO. We assume that intermediates reacting with NO via reaction (3a) will produce MVK and MACR with high-NO_x yields, and intermediates reacting via competing pathways will give NO_x-free yields. Thus, the product yields of MVK and MACR can also be expressed in terms of γ, and the yields under the respective NO_x condition are:

$$\textit{MVK yield} = \gamma \times 0.32 + (1 - \gamma) \times 0.15 \quad (15)$$

$$\textit{MACR yield} = \gamma \times 0.22 + (1 - \gamma) \times 0.18 \quad (16)$$

Thus, the ozone to MVK and ozone to MACR production ratios under "high-NO_x" conditions are (1.9/0.32) = 5.9, and (1.9/0.22) = 8.6, and under "low-NO_x" conditions are (0.79/0.24) = 3.3, and (0.79/0.20) = 3.9, respectively.

[34] While these production ratios would be appropriate for use in calculating the contribution of isoprene to ozone production under conditions of rapid MVK and MACR production, equation (1) will lead to an underestimate of the isoprene contribution if loss becomes significant for either compound. As discussed above, the main isoprene source at this site is 30 km upwind of the measurement site, and while MVK and MACR are produced during transport to the site, the transport time of 2–3 hours is sufficiently long for a significant fraction of each compound to react with OH before reaching Blodgett Forest. To compensate for this effect, we exploit the photochemical properties of MVK and MACR to infer the mean OH level between the isoprene source and the measurement site.

3.6. OH Estimate and Effective Production Ratios From a Simple Model

[35] As discussed in section 3.2.2, the difference between the observed MVK/MACR ratio and the initial production yield ratio from the oxidation of isoprene contains information about the oxidant history of a parcel [*Montzka et al.*, 1993]. Figure 9 shows the observed ΔMVK to ΔMACR ratio for analyzed days in 1998 and 1999. A mean ratio of 2.03 ± 0.04 (standard error) was calculated using mutual least squares regression of the change in MVK over the selected time window against the change in MACR. The change in mixing ratio over the analysis period rather than individual mixing ratio observations was used to reduce the influence of different initial background levels and mixing.

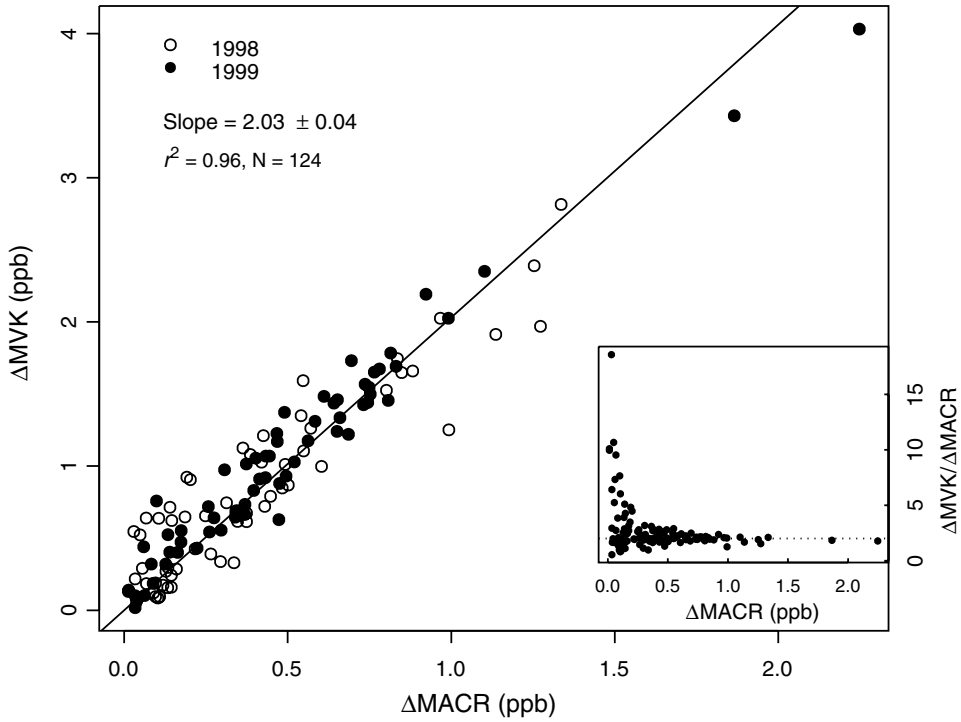

Figure 9. Change in MVK against MACR over the period of simultaneous ozone and isoprene oxidation product increases. The ΔMVK/ΔMACR ratio against ΔMACR is shown in the inset. Each point represents the ratio of the MVK to MACR increase for 1 day in 1998 (empty circles) and 1999 (filled circles).

The effect of horizontal mixing is expected to be small due to the fact that the isoprene source is effectively a line—and not a point—source arrayed perpendicularly to the main wind direction, so that we assume horizontally homogeneous conditions. The effect of vertical mixing, however, depends on the evolution of the mixed layer, and the background MVK to MACR ratio, which is usually around 1 (Figure 7b). The time periods analyzed were selected to avoid periods of rapid boundary layer growth. Tethered balloon measurements by *Greenberg et al.* [1999] over both Oak Ridge, TN, and Pittsboro, NC, indicated that the daytime MVK to MACR ratio remains constant with increasing altitude throughout the mixed layer. Here, we assume that the effect of vertical mixing may reduce the MVK/MACR ratio slightly, but will be small.

[36] The mean upwind [OH] mixing ratio is inferred by comparing the observed ΔMVK to ΔMACR ratio to the ratio of MVK to MACR calculated as a function of [OH] and processing time using a simple zero-dimensional Lagrangian kinetic degradation model. The model had a 6 min time step, and calculated the production and loss of MVK, MACR and ozone from the oxidation of isoprene. Oxidation of isoprene was assumed to be the sole source of MVK and MACR at Blodgett—as evident from the near-zero intercept of their correlation (Figure 6). Both OH and ozone were included as oxidants (without chemical feedback); however, ozone was held at 60 ppb while OH levels were varied from 2 to 14 $\times$ 10^6 molec. cm^{-3}. Surface ozone deposition at a rate of 0.8 cm s^{-1}, and ozone photolysis at a rate of 1 ppb h^{-1}, similar to the ROSE site [*Frost et al.*, 1998], were included as the sole ozone loss processes; however, the effect of deposition was small even if a high deposition velocity of 1.2 cm s^{-1} was assumed [*Bauer et al.*, 2000]. Any photochemical loss of ozone to alkenes is expected to be negligible at the alkene levels encountered. The effect of NO_x on the ozone, MVK, and MACR production yields was also considered, as discussed above.

[37] Isoprene emission from sources between the oak woodland 30 km upwind and the measurement site (herein further called "intermediate sources") can affect the MVK/MACR ratio observed at Blodgett by adding MVK and MACR with a yield ratio of ~1.4 into an aged air mass, thereby reducing the MVK to MACR ratio of that air mass. As discussed previously, a small local isoprene source was detected on hot days (Figure 3a). The existence of such intermediate isoprene sources must, therefore, be considered in the model. The actual level of intermediate isoprene emission will depend on the density and distribution of isoprene emitting species along the air mass trajectory. Three idealized distributions of intermediate isoprene sources were investigated: no intermediate sources, an intermediate source evenly distributed between the oak woodland and the measurement site such that emissions were constant and equal to 10% of the main source, and an intermediate source with exponentially decreasing density scaled such that the isoprene input was 10% of the main source after 2 hours of transport. Both scenarios with intermediate isoprene emission were chosen to reproduce the median isoprene mixing ratio observed at the measurement site of approximately 0.5 ppb (Table 2) after 2.5 hours processing time. In all three cases, the initial isoprene emission was held constant for 45 min to simulate air passing over an approximately 10 km wide band of oak woodlands. While the exact distribution and density of

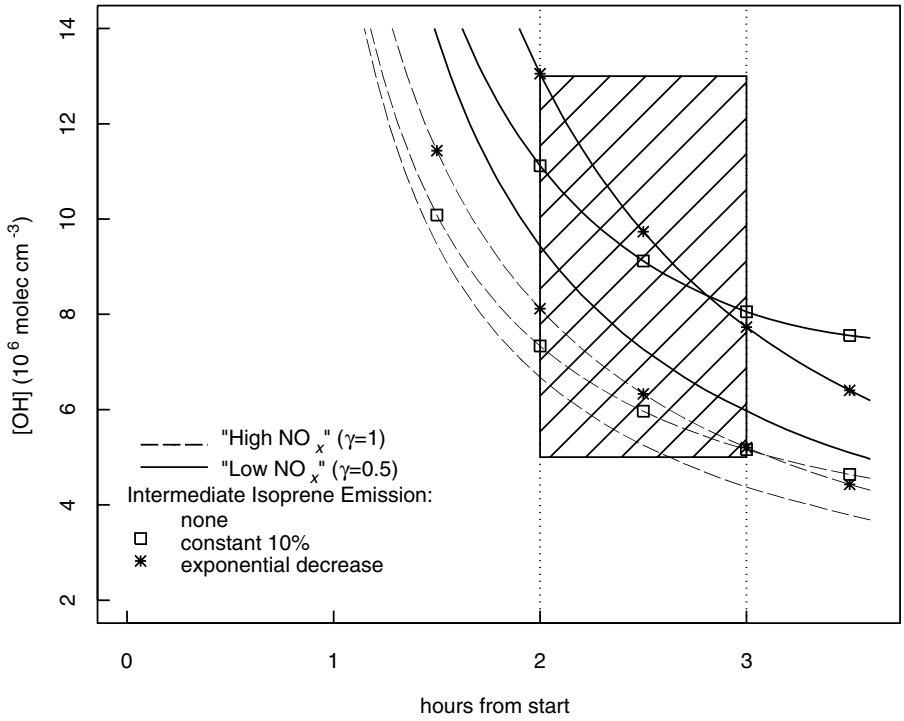

Figure 10. Contour plot of model results giving MVK/MACR = 2 in terms of processing time and [OH]. Hatched box indicates our best guess for mean upwind [OH].

isoprene emitting species along the air mass trajectory is unknown, the chosen emission scenarios attempt to simulate the distribution of actual isoprene emitters between the Sierra foothills and Blodgett Forest (M. Benjamin, California Air Resources Board, personal communication, 2000).

[38] The model results are shown in Figure 10, where each curve represents a combined [OH], processing time, NO_x, and isoprene emission scenario that produces the observed ΔMVK/ΔMACR ratio of $\sim$2. The regular meteorology of the measurement site allows a constraint to be placed on processing time, which is represented by the dotted vertical lines at 2 and 3 hours. The base case of "high-NO_x" conditions (γ = 1) and no intermediate isoprene source corresponds to a mean [OH] of 4–7 $\times$ 106 molec. cm^{-3}. This is approximately 50% lower than recent estimates of the mean [OH] for the Sacramento plume of 11 (±5) $\times$ 106 molec. cm^{-3} [*Dillon et al.*, 2002] and 9–13 (10^6 molec. cm^{-3} [*Schade et al.*, 2002]. Both intermediate isoprene emission sources and "low-NO_x" conditions are required to yield an [OH] of this magnitude, according to our model calculations. The mean [OH] estimated for such cases ranged from 8 to 13 $\times$ 10^6 molec. cm^{-3}, and we will use a mean upwind [OH] of 9 (±4) $\times$ 10^6 molec. cm^{-3} in this study. This estimate (shown by the hatched box in Figure 10) captures the range of [OH] predicted by the model under the scenarios considered, and is in agreement with previous [OH] estimates for the Sacramento plume.

[39] Hydroxyl radical mixing ratios upwind of the measurement site are not expected to be constant over time and space. Depending on whether the center of the Sacramento plume impacts Blodgett or the plume is transported North or South of the site (as occurred on 4 out of 20 days analyzed for July 1997 data [*Dillon et al.*, 2002]), the OH mixing ratios could be as low as 2–4 $\times$ 10^6 molec. cm^{-3}. In addition, wind speed and intermediate emissions may vary from day to day. Intermediate isoprene emissions will vary with temperature and according to season, and at low temperatures, reduced intermediate emissions may explain the observed trend toward increased ΔMVK/ΔMACR ratios at low ΔMACR and ΔMVK (Figure 9, inset).

[40] Assuming a mean upwind OH mixing ratio of 9 (±4) $\times$ 10^6 molec. cm^{-3}, and 2.5 hours processing time, the effective production ratio—the ratio of the net ozone production to the net MVK production calculated by the model—under "high-NO_x" conditions excluding intermediate isoprene emissions was between 12 and 37. Including constant intermediate emissions at 10% of the initial rate gave a range of 11–26 for [OH] = 5–13 $\times$ 10^6 molec. cm^{-3}, and 10–24 for exponentially decreasing intermediate isoprene emissions. The effective production ratio for the "low-NO_x" scenario without intermediate isoprene emissions was between 5.6 and 18, while both intermediate isoprene emission scenarios yielded effective ratios of about 9 ± 4.

[41] Over two-thirds of the measured ozone to MVK slopes were smaller than 30, and a number of days had slopes under 10 (Figure 8). Since the measured slopes should only equal the effective ozone to MVK production ratio when isoprene oxidation is the sole source of ozone production, slopes smaller than the production ratio indicate that less ozone is being formed per MVK than expected, according to the production ratio. Given the importance of intermediate emissions suggested by the comparison of the model results with measured ΔMVK/ΔMACR, and the fact that ambient measurements showed evidence of local isoprene emissions (Figure 3), we adopted effective ozone to

MVK production ratios of 18 ± 8 and 9 ± 4 for our "high-NO_x" and "low-NO_x" cases, respectively. These production ratios are shown as horizontal solid ("low-NO_x") and dashed ("high-NO_x") lines in Figure 8. The effective production ratio for ozone to MACR was also calculated, and best estimates for d[O_3 *isop*]/d[MACR] were 48 ± 28 and 19 ± 11 for our "high-NO_x" and "low-NO_x" cases, respectively. Note that these estimates are 3 and 5 times as high as those calculated using equations (15) and (16), which ignore MVK and MACR losses.

3.7. Trends in the Contribution of Isoprene Oxidation to Ozone Production

[42] Using the d[O_3 *total*]/d[MVK] and our best estimate for the effective ozone to MVK production ratio under "low-NO_x" conditions calculated above, we computed the fraction of total ozone formation attributable to isoprene oxidation at our site for each analyzed day. The contribution of isoprene to ozone concentrations ranged from 3 to over 100% with a median of 34% (49%) for 1998 and 53% (54%) for 1999, assuming "low-NO_x" conditions (median excluding "flagged days" in parentheses). Since 9 of the 10 flagged days were flagged on the basis of changes in [MVK] below the instrument determination limit, indicating that the amount of isoprene oxidized on those days was small, it follows that excluding these days should raise the median we calculate for the contribution of isoprene to ozone production at our site. In the "low-NO_x" scenario, 15 out of the 90 analyzed days had a calculated contribution greater than 100% however, all except one of these days included this maximum based on their individual error estimates. In contrast, 44 out of 90 days in the "high-NO_x" scenario were found to have more than 100% of their ozone formation attributable to isoprene. Since it is not physically possible for isoprene oxidation to account for more than 100% of the observed ozone formation, such a result indicates that less ozone per MVK was being produced from the oxidation of isoprene than the production yield ratio suggests. This means that the ozone to MVK production yield ratio being used is too large. While this could be due to ozone loss being underestimated, or MVK loss being overestimated, low NO_x conditions would also result in a reduced production ratio. Since we find that a greater number of days give greater than 100% isoprene contribution when "high-NO_x" conditions are assumed, this is evidence that "high-NO_x" conditions were generally not present. Isoprene oxidation was found to be the major source of ozone production (over 50% of the total observed ozone increase) on at least 19 out of 44 investigated days in 1998, and 25 out of 46 investigated days in 1999. If most days had experienced "high-NO_x" conditions, then the median isoprene contribution would be greater than 70%, and as many as 31 and 39 of the investigated days in 1998 and 1999, respectively, would have had isoprene as the dominant ozone precursor. No significant differences were found using MACR: 11 out of 36 days in 1998, and 20 out of 45 days in 1999 had greater than 50% isoprene contribution using our best estimate for d[O_3 *isop*]/d[MACR] = 19 ± 11, and the median contribution was at least 30% in both years. These results lend credibility to our analytical method and our understanding of the chemistry involved.

[43] Isoprene oxidation was also a significant source of ozone production on the majority of ozone episode days (maximum [O_3] > 90 ppb). The mean isoprene contribution for 17 ozone episode days in 1998 and 1999 was 77%, assuming "low-NO_x" conditions.

[44] The amount of ozone produced as a result of isoprene oxidation was highly variable. The amount of isoprene oxidized on each particular day could only explain approximately 20% of this variability. Other variables, such as temperature, [NO_x], ozone and PAN chemistry may account for most of the variability observed in the ozone production rates. As shown in Figure 8, the measured slopes tended to decrease, approaching the theoretical production yield limit as the amount of isoprene oxidized (ΔMVK) increased, which indicates that a larger fraction of the observed ozone was attributable to isoprene on days with ample oxidation of isoprene. The isoprene contribution to ozone production also tended to increase exponentially with temperature, as expected based on the exponential temperature dependence of isoprene emissions from plants [*Fuentes et al.*, 2000]. While the correlation between temperature and the isoprene contribution to ozone production was significant ($p < 0.0001$), it could not explain the observed variability ($r^2 = 0.18$). Changing NO_x availability with increasing temperatures may be an important source of this variability. Ozone concentrations have frequently been observed to correlate with temperature [e.g., *Logan*, 1989; *Sillman and Samson*, 1995]. *Sillman et al.* [1990] found that rural ozone concentrations are unlikely to exceed 80 ppb for temperatures below ~290 K, a feature also observed at our site. Model studies have found that this widely observed ozone–temperature relationship is driven in large part by peroxy-acetyl-nitrate (PAN) photochemistry [*Sillman et al.*, 1990; *Sillman and Samson*, 1995]. At higher temperatures NO_x availability is increased due to thermal decomposition of PAN and similar NO_x reservoirs. If this is the case, then conditions at our site may tend to move toward "high-NO_x" conditions on warmer days, increasing the contribution of isoprene oxidation to ozone production on these days. This is supported by the fact that the afternoon decrease in the MVK to MACR ratio thought to indicate increased peroxy-radical competition was not apparent on hot days (maximum temperature > 25°C).

[45] Though the above discussed trends were expected, they were unable to explain a large part of the observed variability. While regional meteorological conditions may explain some additional variance in the calculated contribution of isoprene oxidation to ozone production observed at higher temperatures, their indirect influence on ambient NO_x conditions is probably the most important factor in this analysis. The expansion of Sacramento's urban plume into the Sierra Nevada, as well as its timing, will largely influence the contribution of isoprene's oxidation to ozone formation. However, a more detailed analysis of the variability encountered in this work and of ozone episode days has to be deferred to future analyses.

4. Conclusions

[46] Based on observations of isoprene, its oxidation products MVK and MACR, and ozone, we find that oxidation of isoprene is a major source of ozone production on the

western slope of the Sierra Nevada, CA. Out of approximately 250 total days with observations, the contribution of isoprene oxidation to ozone production was calculated for 44 and 46 mostly summer days in 1998 and 1999, respectively. Contributions were estimated using observed MVK and MACR concentrations, and under both high and low NO_x conditions. The analysis of the measurements of both oxidation products yielded similar estimates for the fraction of ozone production attributable to isoprene, which ranged from 3 to over 100% with a median close to 40%. The contributions estimated assuming "high-NO_x" conditions were substantially higher than those assuming "low-NO_x" conditions, and were frequently above 100%, suggesting that the region generally does not experience "high-NO_x" conditions. However, even assuming "low-NO_x" conditions were the norm, isoprene oxidation was found to be a significant source of ozone production. The consistency of our estimates support our current understanding of isoprene, MVK and MACR photochemistry, in addition to lending credence to our assumptions about [OH] and transport from the primary isoprene emission source.

[47] It should be noted that the slope method described here generally underestimates the total contribution of isoprene to ozone formation, as it only accounts for the ozone produced in the oxidation of isoprene itself. As discussed above, a significant proportion of both MVK and MACR react before reaching Blodgett Forest, and we can assume that an ample portion of the lost isoprene oxidation products have also produced ozone by that time. This secondary ozone production would also more than compensate for chemical and surface deposition ozone losses that we have not addressed in detail.

[48] The ozone/MVK slope analysis revealed that, in general, isoprene's contribution to ozone production increased with increasing isoprene oxidation and temperature, as would be expected. However, the calculated fraction of total daily ozone production attributable to isoprene was highly variable, and could not be adequately explained with the available tracers. The NO_x condition upwind of the measurement site is probably the most important factor determining the ozone production potential of regional isoprene emissions. Meteorology and the amount and timing of advected NO_x from the Sacramento urban plume will significantly influence the amount of ozone produced from isoprene. Along the trajectory from the polluted Sacramento area just 80 km to the southwest of our site, chemistry in the air mass probably transitions from hydrocarbon to NO_x-limited. Our results suggest that the location of this transition will have a strong effect on the ozone production in the region. Integrating our analysis with NO_x and NO_y measurements, and trajectory analyses, may provide a unique opportunity for an observation-based assessment of the effects of NO_x reductions on ozone pollution in the rural environment.

[49] By comparing days with similar meteorology and isoprene emissions, but different [NO_x], we may be able to simulate the effect of upwind NO_x reductions on regional air quality before implementing costly control measures. However, our analysis already shows that only reductions in anthropogenic NO_x emissions, not anthropogenic VOC emissions, may effectively reduce ozone pollution in the Sierra Nevada. Both ample isoprene emissions in the Sierra foothills and high 2-methyl-3-buten-2-ol (MBO) and other VOC emissions from the high Sierra pine forests [*Lamanna and Goldstein*, 1999; *Schade and Goldstein*, 2001] would provide for sufficient ambient VOC mixing ratios to produce ozone even without significant anthropogenic VOC inputs.

Appendix A

[50] Approximately 20 VOCs were routinely measured from the Rtx-WAX column at Blodgett Forest. Some of the dynamically calibrated compounds are listed in Table 1, along with their theoretical response factors, relative to isoprene. Response factors are based on linear least squares calibration lines recorded over multiweek periods.

[51] **Acknowledgments.** This research was supported by grants from the California Air Resources Board (award 98-328), the U.S. Department of Energy (contract DE-AC03-6SF0009), and the University of California Agricultural Experiment Station. G. Dreyfus has been funded by the U.S. Department of Energy Office of Biological and Environmental Research Global Change Education Program (GCEP), Summer Undergraduate Research Experience (SURE), and would like to thank Steve Wofsy for his patient counsel and insight. G. Schade acknowledges funding from the German Academic Exchange Service (DAAD). The authors thank Bob Heald and the Blodgett Forest Crew for their invaluable support, SPI for allowing us to carry out this research on their property, and two anonymous reviewers for their useful comments on the manuscript.

References

Atkinson, R., Atmospheric chemistry of VOCs and NO_x, *Atmos. Environ.*, *34*, 2063–2101, 2000.

Atkinson, R., D. L. Baulch, R. A. Cox, R. F. Hampson Jr, J. A. Kerr, M. J. Rossi, and J. Troe, Summary of evaluated kinetic and photochemical data for atmospheric chemistry, IUPAC Subcommittee on Gas Kinetic Data Evaluation for Atmospheric Chemistry, Web version, December 2000, http://www.iupac-kinetic.ch.cam.ac.uk, 2000.

Barket, D. J., et al., Evaluation of the NO_x dependence of BVOC oxidation using field site data and a simple HO_x model, *Suppl. Eos Trans.*, *81*(48), A11B-29, 2000.

Bauer, M. R., N. E. Hultman, J. A. Panek, and A. H. Goldstein, Ozone deposition to a ponderosa pine plantation in the Sierra Nevada Mountains (CA): A comparison of two different climatic years, *J. Geophys. Res.*, *105*, 22,123–22,136, 2000.

Biesenthal, T. A., and P. B. Shepson, Observations of anthropogenic inputs of the isoprene oxidation products methyl vinyl ketone and methacrolein to the atmosphere, *Geophys. Res. Lett.*, *24*, 1375–1378, 1997.

Biesenthal, T. A., Q. Wu, P. B. Shepson, H. A. Wiebe, K. G. Anlauf, and G. I. Mackay, A study of relationships between isoprene, its oxidation products, and ozone, in the Lower Fraser Valley BC, *Atmos. Environ.*, *31*, 2049–2058, 1997.

Biesenthal, T. A., J. W. Bottenheim, P. B. Shepson, S.-M. Li, and P. C. Brickell, The chemistry of biogenic hydrocarbons at a rural site in eastern Canada, *J. Geophys. Res.*, *103*, 25,487–25,498, 1998.

Bonsangau, B., and C. Boissard, Global distribution of reactive hydrocarbons in the atmosphere, in *Reactive Hydrocarbons in the Atmosphere*, edited by C. N. Hewitt, pp. 209–265, Academic, San Diego, Calif., 1999.

Bowman, F., and J. Seinfeld, Fundamental basis of incremental reactivities of organics in ozone formation in VOC/NO_x mixtures, *Atmos. Environ.*, *28*, 3359–3368, 1994.

Cantrell, C. A., et al., Peroxy radicals as measured in ROSE and estimated from photostationary state deviations, *J. Geophys. Res.*, *98*, 18,355–18,366, 1993.

Carter, W., and R. Atkinson, An experimental study of incremental hydrocarbon reactivity, *Environ. Sci. Technol.*, *21*, 670–679, 1987.

Chameides, W. L., R. W. Lindsay, J. Richardson, and C. S. Kiang, The role of biogenic hydrocarbons in urban photochemical smog: Atlanta as a case study, *Science*, *241*, 1473–1475, 1988.

Chameides, W. L., et al., Ozone precursor relationships in the ambient atmosphere, *J. Geophys. Res.*, *97*, 6037–6055, 1992.

Chen, X., D. Hulbert, and P. B. Shepson, Measurement of the organic nitrate yield from OH reaction with isoprene, *J. Geophys. Res.*, *103*, 25,563–25,568, 1998.

Dillon, M. B., M. S. Lamanna, G. W. Schade, A. H. Goldstein, and R. C. Cohen, Chemical evolution of the Sacramento urban plume: Transport and oxidation, *J. Geophys. Res., 107*(D5), 4239, doi:10.1029/2001JD000696, 2002.

Fehsenfeld, F. C., et al., Emission of volatile organic compounds from vegetation and the implications for atmospheric chemistry, *Glob. Biogeochem. Cycles*, *6*, 389–430, 1992.

Frost, G. J., et al., Photochemical ozone production in the rural southeastern United States during the Rural Oxidants in the Southeastern Environment (ROSE) program, *J. Geophys. Res.*, *103*, 22,491–22,508, 1998.

Fuentes, J. D., et al., Biogenic hydrocarbons in the atmospheric boundary layer: A review, *Bull. Am. Meteorol. Soc.*, *81*(7), 855–867, 2000.

Goldan, P. D., W. C. Kuster, F. C. Fehsenfeld, and S. A. Montzka, Hydrocarbon measurements in the southeastern United States: The rural oxidants in the southern environment (ROSE) program 1990, *J. Geophys. Res.*, *100*, 25,945–25,963, 1995.

Goldstein, A. H., and G. W. Schade, Quantifying biogenic and anthropogenic contributions to acetone mixing ratios in a rural environment, *Atmos. Environ.*, *34*, 4997–5006, 2000.

Goldstein, A. H., M. L. Goulden, J. W. Munger, S. C. Wofsy, and C. D. Geron, Seasonal course of isoprene emissions from a midlatitude deciduous forest, *J. Geophys. Res.*, *103*, 31,045–31,056, 1998.

Goldstein, A. H., N. E. Hultman, J. M. Fracheboud, M. R. Bauer, J. A. Panek, M. Xu, Y. Qi, A. B. Guenther, and W. Baugh, Effects of climate variability on the carbon dioxide, water, and sensible heat fluxes above a ponderosa pine plantation in the Sierra Nevada (CA), *Agric. For. Meteorol.*, *101*, 113–129, 2000.

Goldstein, A. H., G. W. Schade, and G. B. Dreyfus, *Whole Ecosystem Measurements of Biogenic Hydrocarbon Emissions*, Final Report, State of California Air Resources Board, award no. 98-328, 85 pp., 2001.

Greenberg, J. P., A. Guenther, P. Zimmerman, W. Baugh, C. Geron, K. Davis, D. Helmig, and L. F. Klinger, Tethered balloon measurements of biogenic VOCs in the atmospheric boundary layer, *Atmos. Environ.*, *33*, 855–867, 1999.

Grosjean, D., E. L. Williams II, and E. Grosjean, Atmospheric chemistry of isoprene and of its carbonyl products, *Environ. Sci. Technol.*, *27*, 830–840, 1993.

Grossenbacher, J. W., D. J. Barket, K. Ford, P. B. Shepson, T. Thornberry, M. Witmer-Rich, M. A. Carroll, and K. Olszyna, Detailed analysis of the NO_x dependence of isoprene nitrate formation, *Suppl. Eos Trans.*, *81*(48), A11B-30, 2000.

Guenther, A. B., P. R. Zimmerman, P. C. Harley, R. K. Monson, and R. Fall, Isoprene and monoterpene emission rate variability: Model evaluations and sensitivity analyses, *J. Geophys. Res.*, *98*, 12,609–12,617, 1993.

Guenther, A., et al., A global model of natural volatile organic compound emissions, *J. Geophys. Res.*, *100*, 8873–8892, 1995.

Helmig, D., B. Balsley, K. Davis, L. R. Kuck, M. Jensen, J. Bognar, T. Smith Jr., R. V. Arrieta, R. Rodŕguez, and J. Birks, Vertical profiling and determination of landscape fluxes of biogenic nonmethane hydrocarbons within the planetary boundary layer in the Peruvian Amazon, *J. Geophys. Res.*, *103*, 25,519–25,532, 1998.

Jenkin, M. E., A. A. Boyd, and R. Lesclaux, Peroxy radical kinetics resulting from the OH-initiated oxidation of *1*, *3*-butadiene, *2*, *3*-dimethyl-*1,3*-butadiene and isoprene, *J. Atmos. Chem.*, *29*, 267–298, 1998.

Karlik, J. F., and A. M. Winer, Measured isoprene emission rates of plants in California landscapes: Comparison to estimates from taxonomic relationships, *Atmos. Environ.*, *35*, 1123–1131, 2001.

Lamanna, M. S., and A. H. Goldstein, In situ measurements of C_2-C_{10} volatile organic compounds above a Sierra Nevada ponderosa pine plantation, *J. Geophys. Res.*, *104*, 21,247–21,262, 1999.

Logan, J. A., Tropospheric ozone: Seasonal behavior, trends, and anthropogenic influence, *J. Geophys. Res.*, *90*, 10,463–10,482, 1985.

Logan, J. A., Ozone in rural areas of the United States, *J. Geophys. Res.*, *94*, 8511–8532, 1989.

Miyoshi, A., S. Hatakeyama, and N. Washida, OH radical-initiated photooxidation of isoprene: An estimate of global CO production, *J. Geophys. Res.*, *99*, 18,779–18,787, 1994.

Montzka, S. A., M. Trainer, P. D. Goldan, W. C. Kuster, and F. C. Fehsenfeld, Isoprene and it oxidation products, methyl vinyl ketone and methacrolein, in the rural troposphere, *J. Geophys. Res.*, *98*, 1101–1111, 1993.

Montzka, S. A., M. Trainer, W. M. Angevine, and F. C. Fehsenfeld, Measurements of 3-methyl furan, methyl vinyl ketone, and methacrolein at a rural forested site in the southeastern United States, *J. Geophys. Res.*, *100*, 11,393–11,401, 1995.

Paulson, S. E., R. C. Flagan, and J. H. Seinfeld, Atmospheric photooxidation of isoprene, part I, The hydroxyl radical and ground state atomic oxygen reactions, *Int. J. Chem. Kinet.*, *24*, 79–101, 1992a.

Paulson, S. E., R. C. Flagan, and J. H. Seinfeld, Atmospheric photooxidation of isoprene, part II, The ozone–isoprene reaction, *Int. J. Chem. Kinet.*, *24*, 103–125, 1992b.

Reissell, A., and J. Arey, Biogenic volatile organic compounds at Azusa and elevated sites during the 1997 Southern California Ozone Study, *J. Geophys. Res.*, *106*, 1607–1621, 2001.

Roberts, J. M., et al., Measurements of PAN, PPN, and MPAN during the 1994 and 1995 Nashville Intensives of the Southern Oxidant Study: Implications for regional ozone production from biogenic hydrocarbons, *J. Geophys. Res.*, *103*, 22,473–22,490, 1998.

Ruppert, L., and K. H. Becker, A product study of the OH radical-initiated oxidation of isoprene: Formation of C_5-unsaturated diols, *Atmos. Environ.*, *34*, 1529–1542, 2000.

Schade, G. W., and A. H. Goldstein, Fluxes of oxygenated volatile organic compounds from a ponderosa pine plantation, *J. Geophys. Res.*, *106*, 3111–3123, 2001.

Schade, G. W., A. H. Goldstein, and M. S. Lamanna, Are monoterpene emissions influenced by humidity?, *Geophys. Res. Lett.*, *26*, 2187–2190, 1999.

Schade, G. W., A. H. Goldstein, D. W. Gray, and M. T. Lerdau, Canopy and leaf level 2-methyl-3-buten-2-ol fluxes from a ponderosa pine plantation, *Atmos. Environ.*, *34*, 3535–3544, 2000.

Schade, G. W., G. B. Dreyfus, and A. H. Goldstein, Atmospheric methyl-*tertiary*-butyl-ether (MTBE) at a rural mountain site in California, *J. Environ. Qual.*, *31*(4), 1088–1094, 2002.

Sillman, S., The relation between ozone, NO_x and hydrocarbons in urban and polluted rural environments, *Atmos. Environ.*, *33*, 1821–1845, 1999.

Sillman, S., and P. J. Samson, Impact of temperature on oxidant photochemistry in urban, polluted rural and remote environments, *J. Geophys. Res.*, *100*, 11,497–11,508, 1995.

Sillman, S., J. A. Logan, and S. C. Wofsy, The sensitivity of ozone to nitrogen oxides and hydrocarbons in regional ozone episodes, *J. Geophys. Res.*, *95*, 1837–1851, 1990.

Singh, H. B., and P. Zimmerman, Atmospheric distribution and sources of nonmethane hydrocarbons, in *Gaseous Pollutants: Characterization and Cycling*, edited by J. O. Nriagu, 235 pp., John Wiley, New York, 1992.

Starn, T. K., P. B. Shepson, S. B. Bertman, J. S. White, B. G. Splawn, D. D. Riemer, R. G. Zika, and K. Olszyna, Observations of isoprene chemistry and its role in ozone production at a semirural site during the Southern Oxidant Study, *J. Geophys. Res.*, *103*, 22,425–22,435, 1998.

Stevens, P. S., et al., HO_2/OH and RO_2/HO_2 ratios during the Tropospheric OH Photochemistry Experiment: Measurement and theory, *J. Geophys. Res.*, *102*, 6379–6391, 1997.

Stevens, P., D. L'Esperance, B. Chuong, and G. Martin, Measurements of the kinetics of the OH-initiated oxidation of isoprene: Radical propagation in the OH + isoprene + O_2 + NO reaction system, *Int. J. Chem. Kinet.*, *31*, 637–643, 1999.

Stroud, C. A., et al., Isoprene and its oxidation products, methacrolein and methylvinyl ketone, at an urban forested site during the Southern Oxidants Study, *J. Geophys. Res.*, *106*, 8035–8046, 2001.

Trainer, M., E. J. Williams, D. D. Parrish, M. P. Buhr, E. J. Allwine, H. H. Westberg, F. C. Fehsenfeld, and S. C. Liu, Models and observations of the impact of natural hydrocarbons on rural ozone, *Nature*, *329*, 705–707, 1987.

Tuazon, E. C., and R. Atkinson, A product study of the gas-phase reaction of isoprene with the OH radical in the presence of NO_x, *Int. J. Chem. Kinet.*, *22*, 1221–1236, 1990.

Wiedinmyer, C., S. Friedfeld, W. Baugh, J. Greenberg, A. Guenther, M. Fraser, and D. Allen, Measurement and analysis of atmospheric concentrations of isoprene and its reaction products in central Texas, *Atmos. Environ.*, *35*, 1001–1013, 2001.

Yokouchi, Y., Seasonal and diurnal variation of isoprene and its reaction products in a semi-rural area, *Atmos. Environ.*, *28*, 2651–2658, 1994.

G. B. Dreyfus, A. H. Goldstein, and G. W. Schade, Division of Ecosystem Sciences, Department of Environmental Science, Policy, and Management, University of California at Berkeley, 151 Hilgard Hall, Berkeley, CA 94720-3110, USA. (gws@nature.berkeley.edu)